Available online at www.sciencedirect.com
ScienceDirect
Carbohydrate Research 342 (2007) 163–169
Carbohydrate RESEARCH

The fate of β-D-mannopyranose after its formation by endoplasmic reticulum α-(1→2)-mannosidase I catalysis

Chandrika Mulakala,[a,†] Wim Nerinckx[b] and Peter J. Reilly[a,*]

[a]*Department of Chemical and Biological Engineering, 2114 Sweeney Hall, Iowa State University, Ames, IA 50011, USA*
[b]*Department of Biochemistry, Physiology and Microbiology, Ghent University, 9000 Ghent, Belgium*

Received 10 July 2006; received in revised form 26 October 2006; accepted 7 November 2006
Available online 16 November 2006

Abstract—The automated docking program AutoDock was used to dock all 38 characteristic β-D-mannopyranose ring conformers into the active site of the yeast endoplasmic reticulum α-(1→2)-mannosidase I, a Family 47 glycoside hydrolase that converts $Man_9GlcNAc_2$ to $Man_8GlcNAc_2$. The subject of this work is to establish the conformational pathway that allows the cleaved glycon product to leave the enzyme active site and eventually reach the ground-state conformation. Twelve of the 38 conformers optimally dock in the active site where the inhibitors 1-deoxymannonojirimycin and kifunensine are found in enzyme crystal structures. A further 23 optimally dock in a second site on the side of the active-site well, while three dock outside the active-site cavity. It appears, through analysis of the internal energies of different ring conformations, of intermolecular energies between the ligands and enzyme, and of forces exerted on the ligands by the enzyme, that β-D-mannopyranose follows the path $^3E \rightarrow {}^1C_4 \rightarrow {}^1H_2 \rightarrow B_{2,5}$ before being expelled by the enzyme. The highly conserved second site that strongly binds β-D-mannopyranose-$^4C_1$ may exist to prevent competitive inhibition by the product, and is worthy of further investigation.

Keywords: AutoDock; Carbohydrate conformation; Docking; Enzyme mechanism; GH47; Mannose; Mannosidase; Structure–function relationship; Transition state

1. Introduction

Of the hydrolases that process oligosaccharides attached to polypeptides in eukaryotic cells, endoplasmic reticulum α-(1→2)-mannosidase I (ERManI) makes isomer B of $Man_8GlcNAc_2$ from $Man_9GlcNAc_2$ by removing a β-D-mannopyranosyl (β-Man*p*) residue from the middle branch of the oligosaccharide.[1–3] *Saccharomyces cerevisiae*[4] and human[5,6] forms of ERManI, part of glycoside hydrolase Family 47 (GH47),[7] have known tertiary structures. Other α-(1→2)-mannosidase I forms, normally found in the Golgi apparatus, are also GH47 members but have more spacious active sites[8–10] and convert $Man_9GlcNAc_2$ through $Man_6GlcNAc_2$ to $Man_5GlcNAc_2$. All forms have unusual $(\alpha,\alpha)_7$-barrel structures with Ca^{2+} ions at the bases of their active-site wells.

The yeast ERManI crystal structure shows the hydrolytic product $Man_8GlcNAc_2$ isomer B N-linked to one protein molecule and extending into the barrel of the adjacent symmetry-related molecule, interacting with its active site.[4] Human ERManI has been crystallized with no ligands,[5] with the inhibitors 1-deoxymannonojirimycin (DMJ) and kifunensine (KIF),[5] and with the thiodisaccharide substrate analog methyl 2-*S*-(α-D-Man*p*)-2-thio-α-D-Man*p*.[6] DMJ is found as a $^1C_4$ conformer in the same location that the mannosyl residue cleaved from $Man_9GlcNAc_2$ would be expected to occupy,[5] even though its ground-state conformation is $^4C_1$. The thiodisaccharide glycon is in the $^3S_1$ conformation.[6]

We used the automated docking program AutoDock[11] to identify the catalytic base/nucleophile in ERManI. This work also revealed a surprising property of

* Corresponding author. Tel.: +1 515 294 5968; fax: +1 515 294 2689; e-mail: reilly@iastate.edu
† Present address: Department of Chemical Engineering and Materials Science, University of Minnesota, Minneapolis, MN 55455, USA.

0008-6215/$ - see front matter © 2006 Elsevier Ltd. All rights reserved.
doi:10.1016/j.carres.2006.11.012

this enzyme: the active-site funnel is too narrow to allow the passage of the ground-state α-Man*p*-$^4C_1$ glycon having equatorial C-3 hydroxyl and C-5 hydroxymethyl substituents, implying that a conformational change must occur before subsite −1 is occupied.[12] Furthermore, by docking α-D-Man*p*-(1→2)-α-D-Man*p* (α-Man_2) with its glycon in 16 of the 38 possible characteristic ring conformers (Fig. 1) available to aldohexaoses, we established that (1) both $^1C_4$ and $^OS_2$ can be the starting conformers, and these can indeed pass the narrow entry toward the −1 subsite; (2) the most likely binding conformational pathway before the reaction is $(^1C_4 \rightarrow {}^3H_2 \rightarrow)^OS_2 \rightarrow {}^{3,O}B \rightarrow {}^3S_1$; and (3) the subsequent transition state (TS) is close to a ^3E conformation.[13] This is consistent with the observed $^1C_4$ conformations of DMJ and KIF, as well as with the $^3S_1$ glycon conformation of the thiodisaccharide analog observed in the crystal structures. A substitution itinerary that starts from the α-$^3S_1$ conformer is also consistent with the antiperiplanar lone-pair hypothesis (ALPH) of Deslongchamps.[14]

Encouraged by our success in predicting a reasonable α-Man_2 binding pathway before the TS by means of docked energies and forces while holding the enzyme and mannosyl ring structures rigid but allowing exocyclic dihedral angles of the latter to rotate,[13] here we wished to determine the conformational pathway taken by the β-Man*p* product immediately following glycolysis. This query is pertinent, since the ground-state β-$^4C_1$ conformer is also unable to pass the narrow funnel exit from subsite −1. Moreover, three other local minimum conformers have about the same intramolecular energy (E_{Intra}) as β-Man*p*-$^1C_4$,[15] which raises the question of which conformer the enzyme expels. To answer this, we used AutoDock again, this time docking all 38 possible β-Man*p* conformers into the yeast ERManI active site (Protein Data Bank 1DL2) to obtain docked energies. As before,[13] we determined forces on individual atoms of β-Man*p* exerted by the active site to discern how one conformation would be twisted into another along this pathway. We also showed previously[13] how the overall force direction related well with the observed K_I's for DMJ and KIF, where DMJ with a higher K_I was pushed outward from the −1 subsite, whereas KIF was pushed inward. Here we hypothesize that a conformer for which the overall force acting upon it is directed toward the narrow neck of the active-site funnel is more likely to exit the active site.

2. Computational methods

Computational methods were identical to those used earlier.[13] We generated different β-Man*p* conformations with PCModel (Serena Software, Bloomington, IN). Both Lamarkian genetic algorithm (LGA) and pseudo-Solis and Wets local searches[11] within AutoDock were employed to find semioptimal β-Man*p* conformations in the ERManI active site. These were followed by iterative minimization runs with the Solis and Wets local search algorithm.[16] Root mean squared deviations (RMSDs) were calculated from the crystal-structure DMJ molecule in human ERManI, whose active site is almost identical to that of yeast ERManI. Force vectors were calculated from the differences in intermolecular energies on individual ligand atoms over a fine grid divided by the distance between adjacent grid points in *x*, *y*, and *z* directions. Self-consistent Lennard-Jones

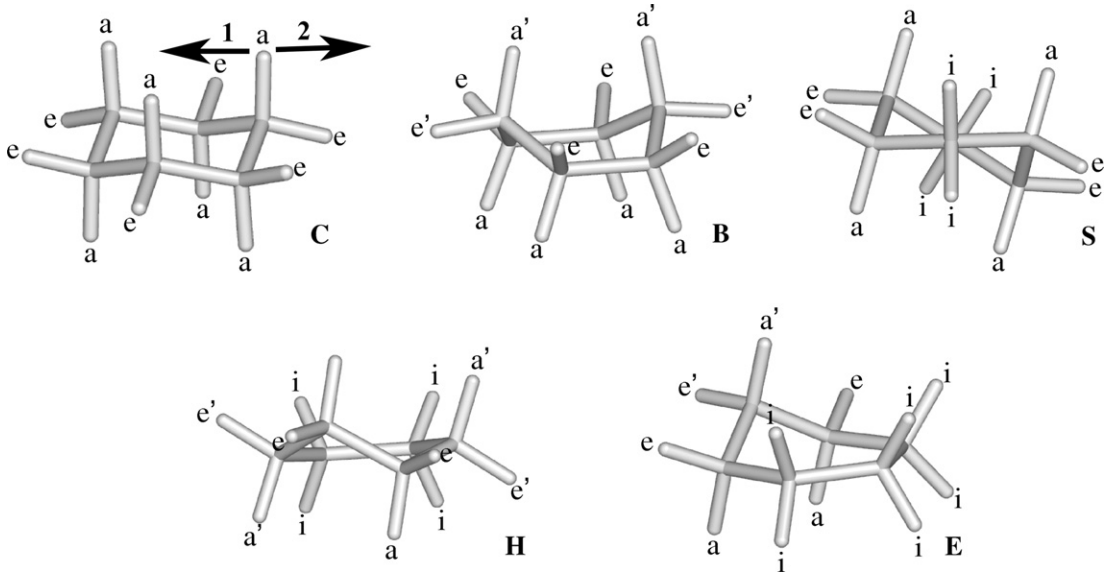

Figure 1. Substituent positions on boat (B), chair (C), envelope (E), half-chair (H), and skew-boat (S) conformations: **a** = axial, **a′** = quasi-axial, **e** = equatorial, **e′** = quasi-equatorial, and **i** = isoclinal.

potentials of AutoDock 1.0 before multiplication by the free-energy model coefficients were used to evaluate nonbonded interaction energies, since they best reproduce the crystal ligands and also because unweighted parameters are necessary to calculate forces on docked ligands. The reported energies are therefore of much higher magnitude than those generated by the AutoDock 3.0 force field, and are representative of binding enthalpies and not free energies.

3. Results and discussion

3.1. Energy computations

The final docked energy reported by AutoDock (E_{Total}) is a sum of the intermolecular interaction energy (E_{Inter}) and the internal energy of the ligand (E_{Intra}). Table 1 shows values of E_{Total}, E_{Inter}, RMSD, and puckering amplitude[17] of all 38 β-Man*p* conformers docked close to crystal-structure DMJ and KIF in subsite −1, where the initially cleaved mannosyl residue would be (Fig. 2). Twelve conformers had their lowest E_{total} values when docked there. Twenty-three conformers optimally docked together some distance from that position, in an indentation on the side of the active-site well (site 2) (Fig. 2). Their energies when docked in this site are shown in Table 1 also, as are those of the three conformers optimally docked much further away (site 3). The best docked energies of ligands that optimally dock in sites 2 or 3 are derived from the LGA, as it allows conformational space to be searched without regard to energy barriers that need to be overcome in moving from one region to another in the grid. The energies and RMSDs of these conformers when docked in subsite −1 are derived from local searches.

As reported previously[13] AutoDock's determination of E_{Intra} is calculated with a simple energy function to reduce computational cost, and it is not sufficiently accurate for direct comparison of E_{Total} values of docked ligands. For instance, the $^{1}C_{4}$ conformer docked in subsite −1 has a more negative E_{Inter} value than the ^{3}E conformer docked there, while the E_{Total} value of the latter is more negative than the former (Table 1). This is highly unlikely since the MM3 force field[15,19] predicts that the $^{1}C_{4}$ conformer has a more negative E_{Intra} value (~7 kcal/mol) than ^{3}E does. However, since an accurate comparison of the docked conformers should ideally be based on E_{Total}, we compared the trends in AutoDock's E_{Inter} values for each ligand conformer with trends in the more accurate E_{Intra} values computed with MM3 (Fig. 3), together with force calculation analysis, to draw conclusions about the product conformational itinerary, similar to the technique we used to predict the conformational itinerary of the substrate to the TS.[13]

Table 1. E_{Total} and E_{Inter} values (kcal/mol), RMSDs (Å), and puckering amplitudes (q, Å) of β-Man*p* ring conformations

Conformer	E_{Total}	E_{Inter}	RMSD	q
Docked in subsite −1				
^{3}E	−105.67	−82.96	0.66	0.48
$^{3}H_{2}$	−102.80	−90.41	0.82	0.50
$^{1}C_{4}$	−100.65	−93.82	0.32	0.50
$^{O}H_{1}$	−98.70	−91.13	2.61	0.58
$^{1}H_{O}$	−98.23	−91.40	0.83	0.49
$^{4}H_{5}$[a]	−98.19	−85.76	2.97	0.57
$^{1}H_{2}$[a]	−96.89	−90.15	0.71	0.51
E_{4}[a]	−96.07	−77.95	2.03	0.50
$^{3,O}B$[a]	−95.87	−87.44	2.70	0.73
$^{5}S_{1}$	−95.72	−88.75	1.10	0.66
$^{2,5}B$	−94.12	−86.41	2.15	0.60
E_{5}[a]	−94.03	−80.85	2.85	0.59
$^{5}H_{O}$	−93.84	−86.12	2.55	0.50
$^{5}H_{4}$	−93.76	−81.02	1.12	0.52
^{4}E[a]	−93.59	−81.34	2.86	0.57
E_{1}	−93.40	−85.51	3.76	0.57
E_{3}[a]	−93.40	−81.64	2.29	0.54
$^{2}H_{3}$[a]	−92.99	−87.55	2.39	0.54
$^{2}S_{O}$[a]	−92.99	−86.62	2.48	0.64
E_{2}[a]	−92.65	−83.41	0.93	0.49
$B_{2,5}$	−92.39	−81.16	3.18	0.72
$^{2}H_{1}$[a]	−92.38	−82.93	2.47	0.53
$^{O}S_{2}$[a]	−92.14	−78.52	2.75	0.76
^{2}E[a]	−91.68	−82.39	2.50	0.53
$^{O}H_{5}$[a]	−90.83	−86.07	4.05	0.59
^{1}E[a]	−90.82	−87.01	0.97	0.54
$^{4}H_{3}$[a]	−90.40	−77.99	2.59	0.55
$^{4}C_{1}$[a]	−90.29	−82.07	2.35	0.59
^{O}E[a]	−90.22	−77.83	3.67	0.59
^{5}E	−89.46	−81.91	1.01	0.51
$^{1}S_{5}$[a]	−89.24	−84.48	3.02	0.76
$^{1}S_{3}$[a]	−87.54	−80.01	2.83	0.74
$^{3}H_{4}$[a]	−87.46	−71.23	1.16	0.51
$B_{3,O}$[a]	−86.63	−77.26	2.41	0.69
$^{3}S_{1}$[a]	−86.39	−80.42	2.51	0.76
$B_{1,4}$[a]	−86.20	−84.51	1.03	0.71
E_{O}[a]	−85.98	−80.72	1.12	0.44
$^{1,4}B$[a]	−80.97	−76.72	6.84	0.70
Optimally docked in site 2				
$^{4}C_{1}$	−110.10	−98.38		0.59
^{O}E	−109.75	−96.16		0.59
$^{1,4}B$	−109.72	−97.55		0.70
$^{4}H_{3}$	−109.29	−96.99		0.55
$^{1}H_{2}$	−105.93	−99.69		0.51
$^{4}H_{5}$	−103.80	−93.08		0.57
E_{2}	−103.53	−85.52		0.49
$^{3}H_{4}$	−102.91	−92.72		0.51
E_{3}	−102.33	−97.65		0.54
^{1}E	−101.80	−96.28		0.54
E_{4}	−100.73	−90.09		0.50
$B_{3,O}$	−100.41	−95.64		0.69
^{2}E	−99.80	−91.51		0.53
$^{2}H_{3}$	−99.43	−90.25		0.54
E_{O}	−98.51	−98.09		0.44
$^{2}H_{1}$	−97.62	−86.88		0.53
$B_{1,4}$	−97.06	−92.16		0.71
$^{3}S_{1}$	−96.94	−90.40		0.76
$^{3,O}B$	−96.71	−88.94		0.73
^{4}E	−96.54	−87.45		0.57
$^{O}H_{5}$	−95.97	−87.90		0.59

(*continued on next page*)

Table 1 (*continued*)

Conformer	E_{Total}	E_{Inter}	RMSD	q
$^{1}S_{5}$	−95.70	−89.00		0.76
$^{1}S_{3}$	−94.26	−94.08		0.74
Optimally docked in site 3				
E_{5}	−105.06	−93.10		0.59
$^{O}S_{2}$	−95.19	−87.46		0.76
$^{2}S_{O}$	−93.66	−75.69		0.64

[a] Optimally docked into sites 2 or 3.

3.2. Force calculations

As in our previous work,[13] force calculations can help to determine the direction of the enzyme-directed conformational twist on the ligand using the following simple intuitive scheme: the torques of the forces on each hydroxyl group were visually examined to establish their effects, as indicated by arrows next to each of the hydroxyl groups in Figure 4. The effects on all five hydroxyl groups were then scored to determine the strength of the twist on the whole ligand. In Figure 1, for example, force **1** causes the C-1 hydroxyl group of β-Man*p*-$^{1}C_{4}$ to remain in the axial position (**a**), whereas force **2** causes it to move toward **a**′, from where it may proceed to **e**, **e**′, or **i** orientations, since they are all consequences of the clockwise torque of force **2**. Therefore, if the force is in direction **1** for a particular transformation, only a C-1 hydroxyl group in the **a** orientation in the final conformer would score 1 point, and all other orientations would score 0 points. For a force in direction **2**, any of the **a**′, **e**, **e**′, or **i** C-1 hydroxyl orientations in the final conformer would score 1 point, while an **a** orientation would score 0 points. This process is repeated for all five OH groups to determine a transformation score for any given conformational change, with the maximal score therefore being 5/5. The transformation scores for conformational changes in the possible pathways appear in Figure 4.

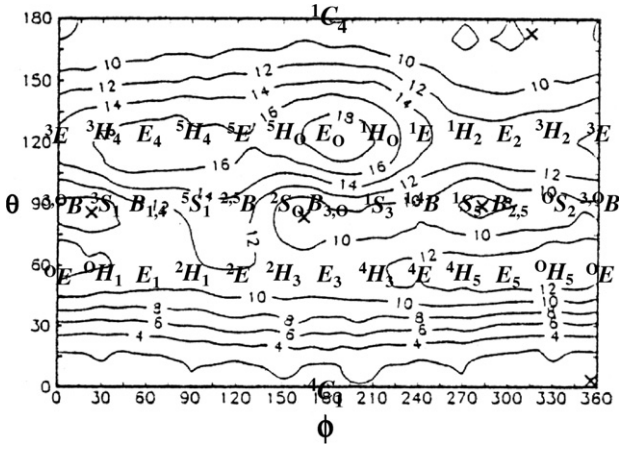

Figure 3. Cremer-Pople isoenergy contour map for β-Man*p*, showing E_{Intra} values in kcal/mol and positions of different conformers.[15] ×'s show local minima, with the global minimum being located near $\theta = 5°$, $\phi = 355°$.

Also, by finding the direction of the overall force vector on the ligands, we can determine whether the ligand on the whole is being pressed against the sides

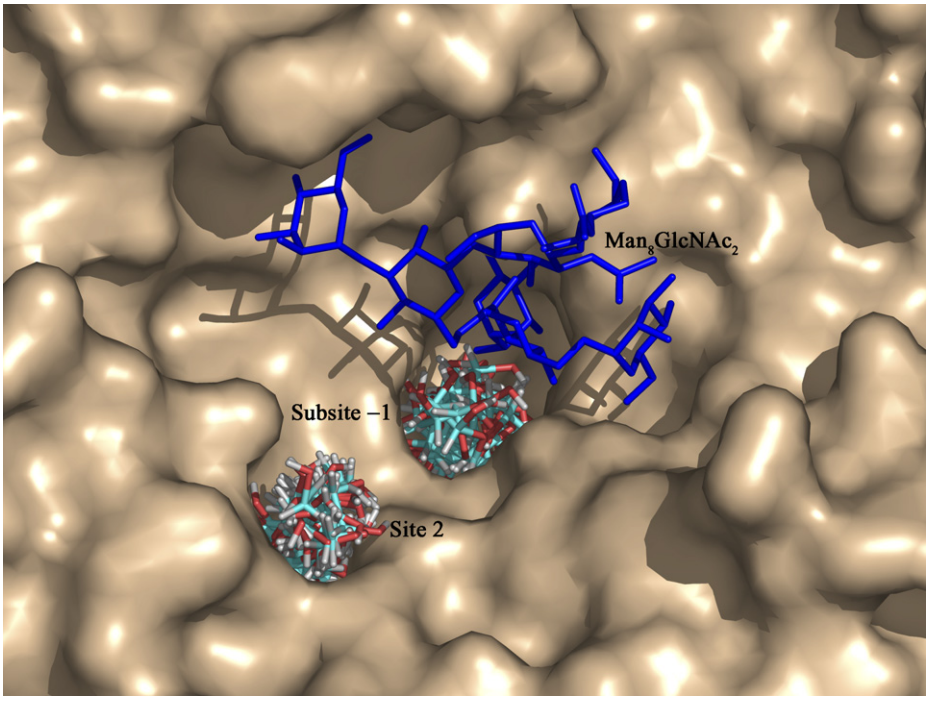

Figure 2. Yeast ERManI active-site region, showing the crystal-structure $Man_8GlcNAc_2$ hydrolytic product (blue), with 12 β-Man*p* molecules docked close to this ligand in subsite −1 and 23 β-Man*p* molecules docked on the side of the active-site well in site 2. Figure rendered with PyMOL.[18]

	^3E	$B_{2,5}$	$^1C_4$	$^3H_2$	$^1H_2$	$^3S_1$
O-1	**i** → **a'**	**a** → **n**	**a** → **a**	**a'** → **i**	**a** → **a**	**e** → **e'**
O-2	**e'** → **n***	**e'** → **i**	**e** → **n**	**e** → **e'**	**e** → **e'**	**i** → **n**
O-3	**a** → **a**	**a** → **a**	**a** → **n**	**a'** → **n**	**a'** → **n**	**a** → **n**
O-4	**a'** → **i**	**e** → **e'**	**a** → **a'**	**i** → **n**	**i** → **e'**	**a** → **a**
O-6	**i** → **e'**	**e** → **e**	**a** → **a'**	**i** → **e'**	**i** → **e'**	**i** → **e**

***n** implies that there is no appreciable force to generate a torque

Transformation scores:

$^3E \rightarrow B_{2,5}$	4/5	$^1C_4 \rightarrow {}^3H_2$	3/5	$^3H_2 \rightarrow B_{2,5}$	1/5
$^3E \rightarrow {}^1C_4$	2/5	$^1C_4 \rightarrow {}^1H_2$	4/5	$^1H_2 \rightarrow B_{2,5}$	3/5
$^3E \rightarrow {}^3S_1$	1/5				

Figure 4. Forces on individual hydroxyl groups of conformations expected to be involved in the product transformation pathway. The orientation of individual hydroxyl groups is indicated (**a** = axial, **a**′ = quasi-axial, **e** = equatorial, **e**′ = quasi-equatorial, and **i** = isoclinal), followed by an arrow showing the effect of that force. Also indicated are the transformation scores for some relevant transformations, for example, 4/5 for $^3E \rightarrow B_{2,5}$ implies that forces on four out of five exocyclic constituents of ^3E drive it toward a $B_{2,5}$ conformation.

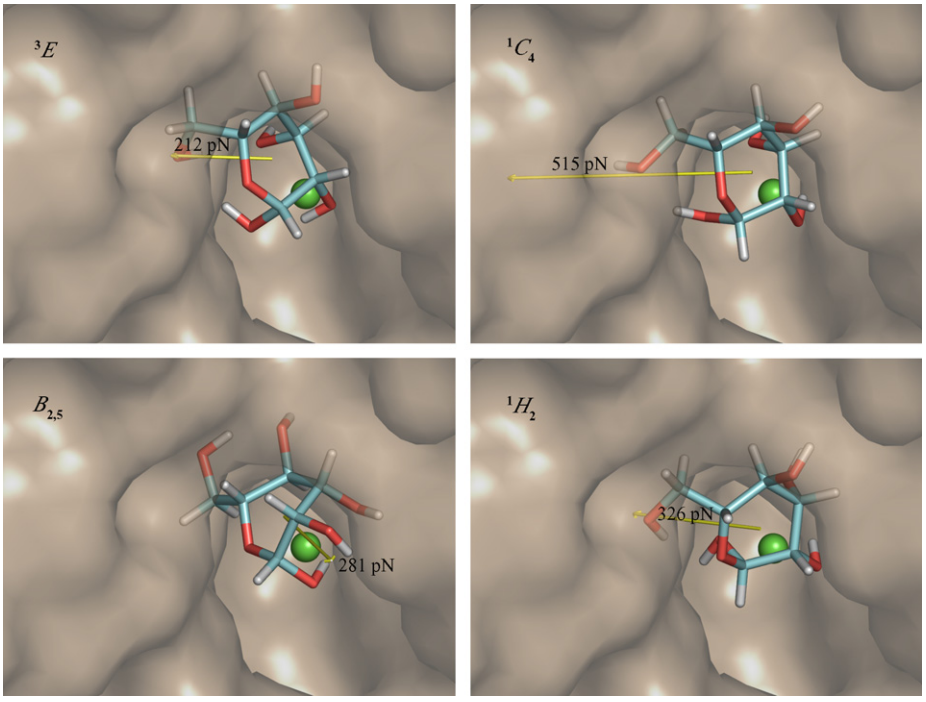

Figure 5. The overall forces on docked ^3E, $^1C_4$, $^1H_2$, and $B_{2,5}$, the four conformers predicted to be involved in product transformation pathway before expulsion from subsite −1. Ca^{2+} at the bottom of the active site is shown as a green sphere. Figure rendered with PyMOL.[18]

or bottom of subsite −1, or whether it is being expelled through the subsite −1 neck. The directions of the overall forces for some important conformers are shown in Figure 5.

3.3. Potential product conformational itineraries

As mentioned earlier, three local minima in the β-Man*p* skew/boat pseudorotational series at $\theta = \sim 90°$ have

E_{intra} values like that of the initially formed $^1C_4$ conformer at $\theta = 173.0°$, $\phi = 314.5°$ (7.16 kcal/mol above the MM3-calculated E_{intra} value of β-Man*p*-$^4C_1$).[15] They are $^1S_5/B_{2,5}$ (6.86 kcal/mol) at $\theta = 89.2°$, $\phi = 282.3°$, $^2S_O/B_{3,O}$ (7.51 kcal/mol) at $\theta = 83.8°$, $\phi = 163.8°$, and $^3S_1$ (7.91 kcal/mol) at $\theta = 86.0°$, $\phi = 22.6°$ (Fig. 3). These three and the $^1C_4$ conformer have overall shapes that are less wide than the ground-state $^4C_1$ conformer with its equatorial C-3 hydroxyl and C-5 hydroxymethyl substituents, so all four can be expelled through the narrow funnel exit from subsite −1.

Of these conformers, $^2S_O/B_{3,O}$ is not directly accessible from ^3E (Fig. 3). ^3E would first have to be transformed to either $^1S_5/B_{2,5}$ or $^3S_1$ and then pseudorotate to $^2S_O/B_{3,O}$. There is a high-energy ridge, caused by a flagpole barrier, between $^3S_1$ and $^2S_O/B_{3,O}$, blocking that pathway. As will be seen below, there is a significant force pushing $B_{2,5}$ out of the active-site pocket, suggesting that the $^2S_O/B_{3,O}$ conformer would be visited rather rarely. Therefore it was not further considered. The docked E_{Inter} and RMSD values for $^1C_4$, $^1S_5/B_{2,5}$, and $^3S_1$ are −93.82, −81.16/−84.45, and −80.42 kcal/mol and 0.66, 3.02/3.18, and 2.51 Å, respectively (Table 1). Since the $B_{2,5}$ docks with a lower E_{Inter} value than $^1S_5$, and also docks optimally in site 1 ($^1S_5$ optimally docks in site 2), we will henceforth consider the docked $B_{2,5}$ conformer to be representative of the $^1S_5/B_{2,5}$ local minimum seen on the MM3 isoenergy surface (Fig. 3). The $^1C_4$ conformer with its low E_{Inter} and RMSD values seems to be the most likely destination for the newly formed product. However, the forces on ^3E seem to suggest that its transformation to a $B_{2,5}$-like conformer is more likely than its transformation to $^1C_4$. Also, the overall force on the $B_{2,5}$ conformer is toward the active-site neck, whereas the $^1C_4$ conformer seems pushed sideward (Fig. 5). Since the $^1C_4$ conformer also has the lowest E_{Inter} value of all the conformers docked in subsite −1, it is tempting to speculate that the ^3E-like product is directly pushed toward the $^1S_5/B_{2,5}$ minimum to prevent it from getting trapped in the lowest-energy $^1C_4$ conformer, which, based on the overall force (Fig. 5), cannot directly leave the active site. Since all other conformers dock with higher energy than the $^1C_4$ conformer, it would seem that thermal excitation energy would have to be involved in further transformations for the product to escape from the active site; the enzyme–product system would not merely be relaxing to a lower potential energy state, as was observed in the transformation of the enzyme–substrate system to the enzyme–TS system.[13]

However, theoretical considerations point toward an initial collapse of the transient TS species to a $^1C_4$ conformation. Enzymatically catalyzed glycopyranoside substitution itineraries do not operate through a discrete carbocation in a first-order reaction, but are borderline SN_1–SN_2, since recently observed primary ^{13}C[20,21] as well as secondary α-deuterium[22] kinetic isotope effects are consistent with SN_2-type pathways. In such reaction pathways, the TS is a transient species with an ultrashort lifetime.[23] For reaction itineraries catalyzed by GH47 members, the conformer resulting immediately after the ^3E-TS is very likely the β-$^1C_4$ inverted chair, as conversion of the α-$^3S_1$-pre-TS conformer into the ^3E-TS conformer and a subsequent slight further atomic displacement in the same direction following the principle of least motion[24] leads to a collapse into the β-Man*p*-$^1C_4$ conformer. It appears at first strange that the end of this collapse is the inverted chair, which carries two unfavorable *syn*-diaxial substituent positionings (from the C-3 hydroxyl and C-5 hydroxymethyl groups) toward the β-axial anomeric hydroxyl group, whereas these are not present toward the incoming water nucleophile at the stage of the transient TS. However, the newly formed β-product at the start of the collapse, very shortly after the TS, still resembles the TS, according to the Hammond postulate, and does not yet experience the steric repulsions that it will encounter at the end of the collapse. Hence, the collapse will be in the direction of the inverted chair, since this is a least-atomic-motion movement that also provides maximal initial ring strain release, irrespective of the steric situation at the end of the collapse. Further travel away from the $^1C_4$ conformer then depends on the energy barriers needed to be transversed and the forces exerted by subsite −1 on the ligand and its individual atoms.

A conformational change of the initially formed β-Man*p*-$^1C_4$ into the skew/boat pseudorotational series should proceed through a conformer in the $\phi = 270$–330° saddle point of the half-chair/envelope pseudorotational series at $\theta = \sim 120°$, which can be either $^1H_2$ or $^3H_2$ based on their E_{Inter} values of −90.15 and −90.41 kcal/mol, respectively (Table 1). Based on the forces on these two conformers and $^1C_4$, $^1H_2$ seems to be the more likely intermediate conformer with a further transition to the $B_{2,5}/^1S_5$ local minimum. The overall forces on the $^1H_2$ and $B_{2,5}$ conformers (Fig. 4) indicate that only the latter is capable of exiting the active site.

3.4. Product binding site

Site 2 is highly conserved, its tertiary structure being the same in both *S. cerevisiae* and human forms of ER-ManI. There are 12 amino acid residues (Asp61, Val62, Tyr63, Met73, Trp82, Ile83, Arg136, Asn495, Met496, Glu497, Ser498, and Phe499 in *S. cerevisiae* ERManI numbering) within 4 Å of Man*p*-$^4C_1$ docked in site 2. Seven of them (Asp61, Met73, Trp82, Ile83, Glu497, Ser498, and Phe499) are conserved in *Candida albicans*, human, and *S. cerevisiae* ERManIs, the only three ER-ManI forms with known sequences, and the last three residues are conserved over a large range of GH47 members. This factor, as well as the fact that 23 of the

β-Man*p* conformers have more negative E_{Total} and E_{Inter} values when bound in site 2 rather than when bound in subsite −1, suggest that subsite 2 may play a major role in ERManI function.

Molecules of β-Man*p* leaving subsite −1 would quickly reach the ground-state β-Man*p*-$^4C_1$ conformer and would slowly mutarotate into an equilibrium mixture of 64% α-Man*p* and 36% β-Man*p*, with only very small amounts of the furanosyl ring form.[25,26] Site 2 binds β-Man*p*-$^4C_1$ much better than does subsite −1 (where DMJ and KIF are bound), as evidenced by the E_{Inter} values of forms bound in the two locations (Table 1). Along with subsite −1, ERManI has several other mannose-binding subsites that are clearly observed when $Man_8GlcNac_2$ is bound by *S. cerevisiae* ERManI (Fig. 2), all of which bind α-mannosyl residues in the $^4C_1$ conformer, and which no doubt confer high substrate selectivity on the enzyme. The expelled mannose from subsite −1 after catalysis could potentially be bound by any of these subsites, thus interfering with substrate binding for further catalytic cycles. The fact that site 2 does not overlap with any of these subsites may imply that it is designed to keep the product away from substrate-binding subsites to prevent product inhibition.

There is no evidence that site 2 has been previously observed. However, in none of the five different GH47 enzymes that have been crystallized was mannose part of the crystallizing solution or was it soaked into the crystals. Therefore mannose molecules would be unlikely to appear in site 2 in the crystal structure, as in addition they were not found in the subsites where the substrate would be productively bound. In several cases DMJ and KIF were found in crystal structures of the active site, but not in site 2, perhaps because they cannot be bound by it.

In any case, further investigation of site 2 through crystallographic and mutagenetic studies may be worth pursuing.

4. Conclusions

Twelve of the 38 possible conformers of β-Man*p*-$^1C_4$ optimally docked in subsite −1 of the active site, while 23 optimally docked in a second site on the side of the active-site well and three did not dock within the well. Theoretical considerations indicate that the ^3E-TS conformer is first transformed to the $^1C_4$ conformer. Analysis of E_{Inter} and E_{Intra} values, forces, and RMSDs of conformers docked in subsite −1 suggest that the subsequent pathway of β-Man*p* is through the $^1H_2$ saddle point to the low-E_{Intra} $^1S_5/B_{2,5}$ conformer before it is expelled from the active site. The strongly conserved second site much more tightly binds β-Man*p*-$^4C_1$ than does subsite −1, suggesting that mannose from the aqueous solution would not be bound in the latter site to competitively inhibit substrate binding by ERManI.

Acknowledgments

We thank Professor Arthur Olson (Scripps Research Institute) for donating AutoDock and gratefully acknowledge financial support from the US National Science Foundation.

References

1. Herscovics, A. *Biochim. Biophys. Acta* **1999**, *1426*, 275–285.
2. Herscovics, A. *Biochim. Biophys. Acta* **1999**, *1473*, 96–107.
3. Herscovics, A. *Biochimie* **2001**, *83*, 757–762.
4. Vallée, F.; Lipari, F.; Yip, P.; Sleno, B.; Herscovics, A.; Howell, P. L. *EMBO J.* **2000**, *19*, 581–588.
5. Vallée, F.; Karaveg, K.; Herscovics, A.; Moremen, K. W.; Howell, P. L. *J. Biol. Chem.* **2000**, *275*, 41287–41298.
6. Karaveg, K.; Siriwardena, A.; Tempel, W.; Liu, Z. J.; Glushka, J.; Wang, B.-C.; Moremen, K. W. *J. Biol. Chem.* **2005**, *280*, 16197–16207.
7. Coutinho, P. M.; Henrissat, B. 1999. <http://afmb.cnrs-mrs.fr/CAZY/>.
8. Van Petegem, F.; Contreras, H.; Contreras, R.; Van Beeumen, J. *J. Mol. Biol.* **2001**, *312*, 157–165.
9. Lobsanov, Y. D.; Vallée, F.; Imberty, A.; Yoshida, T.; Yip, P.; Herscovics, A.; Howell, P. L. *J. Biol. Chem.* **2002**, *277*, 5620–5630.
10. Tempel, W.; Karaveg, K.; Liu, Z.-J.; Rose, J.; Wang, B.-C.; Moremen, K. W. *J. Biol. Chem.* **2004**, *279*, 29774–29786.
11. Morris, G. M.; Goodsell, D. S.; Halliday, R. S.; Huey, R.; Hart, W. E.; Belew, R. K.; Olson, A. J. *J. Comput. Chem.* **1998**, *19*, 1639–1662.
12. Mulakala, C.; Reilly, P. J. *Proteins* **2002**, *49*, 125–134.
13. Mulakala, C.; Nerinckx, W.; Reilly, P. J. *Carbohydr. Res.* **2006**, *341*, 2233–2245.
14. Deslongchamps, P. *Pure Appl. Chem.* **1993**, *65*, 1161–1178.
15. Dowd, M. K.; French, A. D.; Reilly, P. J. *Carbohydr. Res.* **1994**, *264*, 1–19.
16. Solis, F. J.; Wets, R. J.-B. *Math. Operat. Res.* **1981**, *6*, 19–30.
17. Spek, A. L. *J. Appl. Cryst.* **2003**, *36*, 7–13. <http://www.cryst.chem.uu.nl/platon>.
18. PyMOL, DeLano Scientific, South San Francisco, Cal. <http://www.pymol.org>.
19. Allinger, N. L.; Yuh, Y. H.; Lii, J.-H. *J. Am. Chem. Soc.* **1989**, *111*, 8551–8566.
20. Huang, X.; Tanaka, K. S. E.; Bennet, A. J. *J. Am. Chem. Soc.* **1997**, *119*, 11147–11154.
21. Berti, P. J.; Tanaka, K. S. E. *Adv. Phys. Org. Chem.* **2002**, *37*, 239–314.
22. Vocadlo, D. J.; Wicki, J.; Rupitz, K.; Withers, S. G. *Biochemistry* **2002**, *41*, 9727–9735.
23. Kurzynski, M. *FEBS Lett.* **1993**, *328*, 221–224.
24. Hine, J. *Adv. Phys. Org. Chem.* **1977**, *15*, 1–61.
25. Angyal, S. J. *Adv. Carbohydr. Chem. Biochem.* **1984**, *42*, 15–68.
26. Angyal, S. J. *Adv. Carbohydr. Chem. Biochem.* **1991**, *49*, 19–35.